

Local structure in nematic and isotropic liquid crystals

Nguyen Hoang Phuong and Friederike Schmid

Fakultät für Physik, Universität Bielefeld, 33615 Bielefeld, Germany

By computer simulations of systems of ellipsoids, we study the influence of the isotropic/nematic phase transition on the direct correlation functions (DCF) in anisotropic fluids. The DCF is determined from the pair distribution function by solving the full Ornstein-Zernike equation, without any approximations. Using a suitable molecular-fixed reference frame, we can distinguish between two qualitatively different contributions to the DCF: One which preserves rotational invariance, and one which breaks it and vanishes in the isotropic phase. We find that the symmetry preserving contribution is barely affected by the phase transition. However, symmetry breaking contributions emerge in the nematic phase and may become quite substantial. Thus the DCF in a nematic fluid is not rotationally invariant. In the isotropic fluid, the DCF is in good agreement with the prediction of the Percus-Yevick theory.

I. INTRODUCTION

The pair direct correlation function (DCF) is a central quantity in the theory of liquids. Through the Ornstein-Zernike relation¹, it is related to the pair distribution function, which is accessible experimentally. Compared to the latter, it often has a much simpler structure, because the Ornstein-Zernike relation eliminates to a large extent the contributions of third particles to the pair correlations. Moreover, the DCF plays a key role in density functional theories, since it is the second functional derivative of the excess free energy with respect to the local density^{1,2}. Much effort has therefore been devoted to the investigation of DCFs in molecular fluids.

Most studies have considered isotropic fluids: Early integral equation approaches are due to Wulf⁷, and Chen and Steele⁶. Chen and Steele generalized the Ornstein-Zernike equation to the case of particles with orientation dependent interactions^{6,31} and calculated the structure of diatomic fluids using a Percus-Yevick⁴ closure. Percus-Yevick and Hypernetted Chain¹ theories for isotropic fluids with orientation dependent interactions have also been introduced by Pynn⁵, Fries and Patek⁸, and Singh and coworkers⁹. Several authors have calculated DCFs in isotropic liquid crystals using theories of this kind^{5,10-13}. The resulting pair correlation functions were generally in reasonable agreement with available simulation data.

Alternative approaches have been pursued, e. g., by Wulf^{7,14}, Rickayzen and coworkers¹⁵⁻¹⁷, and Chamoux and Perera¹⁸. Rickayzen et al choose a geometrically motivated Ansatz for the form of the DCF and optimize the parameters such that the Percus-Yevick relation is fulfilled in a given limit. Chamoux and Perera derive approximations for the DCF from the Rosenfeld density functional¹⁹. For fluids of elongated particles, their DCF is similar to that obtained with the Percus-Yevick or Hypernetted chain calculations of Perera et al¹⁰. A number of other authors have suggested simple approximate expressions for the DCF in isotropic molecular fluids^{5,14,21-24}. Some of these fit simulation data surpris-

ingly well²⁵. The direct determination of the DCF from computer simulations is rather tedious. Allen et al²⁵ have presented a method which allows to calculate the DCF from pair correlation data, and applied it to study the DCF in fluids of ellipsoids²⁵ and of Gay-Berne²⁶ particles^{27,28}.

The DCF has thus been studied quite intensely in isotropic fluids. In contrast, only few studies have considered the DCF in anisotropic, e. g., nematic fluids. In a nematic liquid crystal, the particles remain positionally disordered, but align preferentially along one (arbitrary) direction^{29,30}. The isotropy of space is spontaneously broken. Consequently, the pair correlation functions lose their rotational invariance. Moreover, soft Goldstone modes must be present, since the orientational order breaks a continuous symmetry: The structure factor diverges in the $\mathbf{k} \rightarrow 0$ limit, and the pair distribution function exhibits a long range elastic tail. This implies that the DCF must fulfill certain conditions in the $\mathbf{k} \rightarrow 0$ limit, which have been derived by Gubbins³¹, and later in a different manner by Zhong and Petschek³².

Workman and Fixman³³ have formulated the general form of the Ornstein-Zernike equation for the case of anisotropic fluids. They also suggested a Percus-Yevick closure which is based on a density functional about an isotropic reference state, but can be applied to both isotropic and anisotropic liquids. In fact, the Percus-Yevick and the Hypernetted chain closure lend themselves to a rather straightforward generalization for anisotropic fluids³⁴. Caillol and coworkers³⁴ have used these closures to calculate the structure of perfectly aligned fluids. Zhong and Petschek³² have analyzed the diagrammatic expansion of the DCF in this approach, and proved that at least the Percus-Yevick closure must fail to reproduce the soft Goldstone modes in the general case of spontaneous partial order. In order to fix the problem without resorting to a reference state, they proposed a modified Percus-Yevick closure which premises

that the DCF is rotationally invariant. Given that the DCF is vaguely related to an “effective interaction potential” between particles^{4,32}, this assumption seems plausible. Nevertheless, a clearcut test of the hypothesis is clearly desirable.

In practice, theoretical studies of DCFs in partially ordered nematic fluids have mostly been concerned with systems with separable interactions^{35,36}, where the interparticle potential depends on the spatial separation and the orientation of particles independently. Very little is still known on the DCF in general anisotropic fluids. Simulation studies have been performed by Stelzer et al³⁷ (nematic Gay-Berne fluids), and by Zakharov and Maliniak³⁸ (5CB molecules). These authors used an “unoriented nematic approximation”, which replaces the pair correlations by their rotational averages. The simplification has later been questioned by Longa et al³⁹. Indeed, the elastic properties of the nematic fluid, which can be calculated from the DCF using the Poniewierski-Stecki equations⁴⁰, don’t seem to be captured very well⁴¹. Moreover, an analysis which uses such an approximation is clearly not suited to elicit whether or not the DCF depends on the direction of preferred alignment in the nematic fluid.

In a previous paper⁴², we have presented a method for determining the DCF in uniaxial nematic fluids without approximations from computer simulations. As a test of the method, we have applied it to a nematic fluid of soft ellipsoids and calculated the elastic constants from the DCF via the Poniewierski-Stecki equations⁴⁰. The results were in good agreement with those obtained independently from an analysis of order tensor fluctuations, following a procedure by Allen et al⁴¹. Thus we have shown that the method takes into account the elastic properties of the fluid in an adequate way.

In the present work, we use our method to analyze the form of the DCF in detail for different state points in the nematic and the isotropic phase. In particular, we discuss the symmetry properties and the range of the DCF, the pair distribution function, and the total correlation function. We show that the DCF is truly short ranged as expected. The elastic tails and the near-critical long range fluctuations close to the nematic-isotropic transition disappear. On the other hand, our data show that the DCF does reflect the broken symmetry of the nematic phase, and the assumption of rotational invariance is not correct in our system.

The paper is organized as follows: In the next section, we define the simulation model, introduce the pair correlation functions and explain how we perform the data analysis. The results are presented and discussed in section III. In the isotropic phase, we compare them with the prediction of the Percus-Yevick theory. Some comments on the Percus-Yevick solution and how it breaks down at large densities are added in the appendix. We summarize and conclude in section IV.

II. MODEL AND METHOD

A. simulation model

We have studied a fluid of soft ellipsoidal particles with repulsive pair interactions

$$V_{12} = \begin{cases} 4\epsilon_0 (X_{12}^{12} - X_{12}^6) + \epsilon_0 & : X_{12}^6 > 1/2 \\ 0 & : \text{otherwise} \end{cases} \quad (1)$$

The function $X_{12} = \sigma_0 / (r_{12} - \sigma_{12} + \sigma_0)$ depends on the distance r_{12} between particles 1 and 2, and on the shape function⁴³

$$\sigma_{12}(\mathbf{u}_1, \mathbf{u}_2, \hat{\mathbf{r}}_{12}) = \sigma_0 \left\{ 1 - \frac{\chi}{2} \left[\frac{(\mathbf{u}_1 \cdot \hat{\mathbf{r}}_{12} + \mathbf{u}_2 \cdot \hat{\mathbf{r}}_{12})^2}{1 + \chi \mathbf{u}_1 \cdot \mathbf{u}_2} + \frac{(\mathbf{u}_1 \cdot \hat{\mathbf{r}}_{12} - \mathbf{u}_2 \cdot \hat{\mathbf{r}}_{12})^2}{1 - \chi \mathbf{u}_1 \cdot \mathbf{u}_2} \right] \right\}^{-1/2}, \quad (2)$$

which approximates the contact distance between two ellipsoids of elongation $\kappa = \sqrt{(1 + \chi)/(1 - \chi)}$ with orientations \mathbf{u}_1 and \mathbf{u}_2 and center-center vector \mathbf{r}_{12} pointing in the direction $\hat{\mathbf{r}}_{12} = \mathbf{r}_{12}/r_{12}$. The parameters were $\kappa = 3$ and $k_B T = 0.5\epsilon_0$.

Four state points were considered, two at densities $\rho = 0.24/\sigma_0^3$ and $0.283/\sigma_0^3$ in the isotropic phase, and two at densities $0.287/\sigma_0^3$ and $\rho = 0.3/\sigma_0^3$ in the nematic phase. The system size was $N = 1000$ particles at $\rho = 0.24/\sigma_0^3$, $N = 4000$ at $\rho = 0.283/\sigma_0^3$ and $0.287/\sigma_0^3$, and $N = 1000 - 8000$ at $\rho = 0.3/\sigma_0^3$. The systems with the three lower densities were studied in the canonical ensemble by Monte Carlo simulation. The data for the larger systems ($N \geq 4000$) at the density $\rho = 0.3\sigma_0^{-3}$ were originally produced by G. Germano⁴². They were simulated in the microcanonical ensemble using a parallel molecular dynamics program on a CRAY T3E. Here the moment of inertia of a particle was chosen $I = 2.5m_0\sigma_0^2$ and the time step $\Delta t = 0.003\sigma_0\sqrt{m_0/\epsilon_0}$, where m_0 is the mass of one particle. The results did not depend on the simulation method. Run length were 5-10 million MC or MD steps, depending on the system size, and data were collected every 1000 or 10000 steps.

Throughout this paper, the units will be defined in terms of the energy unit ϵ_0 , the mass unit m_0 , the temperature unit ϵ_0/k_B , and the length unit σ_0 .

The orientational order is characterized as usual by the order tensor²⁹

$$\mathbf{Q} = \left\langle \frac{1}{N} \sum_{i=1}^N \left(\frac{3}{2} \mathbf{u}_i \otimes \mathbf{u}_i - \frac{1}{2} \mathbf{I} \right) \right\rangle, \quad (3)$$

where the sum i runs over all N particles of orientation \mathbf{u}_i , \mathbf{I} is the unit matrix, \otimes the dyadic vector product, $\langle \cdot \rangle$ denotes thermal averages. The largest eigenvalue of \mathbf{Q} is the nematic order parameter VP_2 , and the corresponding eigenvector \mathbf{n} is the director, which points along the direction of preferred alignment. In our case, we have

$P_2 = 0.47$ at $\varrho = 0.287/\sigma_0^3$, and $P_2 = 0.69$ at $\varrho = 0.3/\sigma_0^3$. The densities $\varrho = 0.283/\sigma_0^3$ and $\varrho = 0.287/\sigma_0^3$ are close to the coexisting densities at the isotropic/nematic phase transition. Previous constant pressure simulations of the same system⁴⁴ showed that the transition is only very weakly first order, and the width of the coexistence gap is of the order of $0.05/\sigma_0^3$.

B. Data analysis

Before describing our way to analyze the data, we recall some basic definitions: In a system of particles i with orientation \mathbf{u}_i and position \mathbf{r}_i , the one-particle distribution can be written as¹

$$\rho^{(1)}(\mathbf{u}, \mathbf{r}) = \left\langle \sum_i \delta(\mathbf{u} - \mathbf{u}_i) \delta(\mathbf{r} - \mathbf{r}_i) \right\rangle. \quad (4)$$

and the pair distribution as

$$\begin{aligned} \rho^{(2)}(\mathbf{u}_1, \mathbf{r}_1, \mathbf{u}_2, \mathbf{r}_2) \\ = \left\langle \sum_{i \neq j} \delta(\mathbf{u}_1 - \mathbf{u}_i) \delta(\mathbf{r}_1 - \mathbf{r}_i) \delta(\mathbf{u}_2 - \mathbf{u}_j) \delta(\mathbf{r}_2 - \mathbf{r}_j) \right\rangle. \end{aligned} \quad (5)$$

In homogeneous nematic fluids, the pair distribution depends on the difference vector $\mathbf{r}_{12} = \mathbf{r}_1 - \mathbf{r}_2$ rather than on the individual positions \mathbf{r}_1 and \mathbf{r}_2 , and the single-particle distribution depends only on \mathbf{u} (in fact, on $|\mathbf{u} \cdot \mathbf{n}|$). In that case, the total correlation function $h(\mathbf{u}_1, \mathbf{u}_2, \mathbf{r}_{12})$ is defined by

$$h(\mathbf{u}_1, \mathbf{u}_2, \mathbf{r}_{12}) = \frac{\rho^{(2)}(\mathbf{u}_1, \mathbf{u}_2, \mathbf{r}_{12})}{\rho^{(1)}(\mathbf{u}_1)\rho^{(1)}(\mathbf{u}_2)} - 1, \quad (6)$$

and the direct correlation function $c(\mathbf{u}_1, \mathbf{u}_2, \mathbf{r}_{12})$ is determined by the Ornstein-Zernike equation^{1,3,33}

$$\begin{aligned} h(\mathbf{u}_1, \mathbf{u}_2, \mathbf{r}_{12}) = c(\mathbf{u}_1, \mathbf{u}_2, \mathbf{r}_{12}) + \\ \int c(\mathbf{u}_1, \mathbf{u}_3, \mathbf{r}_{13}) \rho^{(1)}(\mathbf{u}_3) h(\mathbf{u}_3, \mathbf{u}_2, \mathbf{r}_{32}) d\mathbf{u}_3 d\mathbf{r}_3. \end{aligned} \quad (7)$$

We choose a coordinate frame where the z axis points in the direction of the director \mathbf{n} (director frame)⁴⁵. All orientation dependent functions are expanded in spherical harmonics $Y_{lm}(\mathbf{u})$. This yields

$$\rho^{(1)}(\mathbf{u}) = \varrho \sum_{l \text{ even}} f_l Y_{l0}(\mathbf{u}), \quad (8)$$

with the bulk number density ϱ , and

$$\begin{aligned} F(\mathbf{u}_1, \mathbf{u}_2, \mathbf{r}) = \sum_{\substack{l_1, l_2, l \\ m_1, m_2, m}} F_{l_1 m_1 l_2 m_2 l m}(r) \\ Y_{l_1 m_1}(\mathbf{u}_1) Y_{l_2 m_2}(\mathbf{u}_2) Y_{l m}(\hat{\mathbf{r}}), \end{aligned} \quad (9)$$

where F stands for $\rho^{(2)}$, h or c , and $\hat{\mathbf{r}}$ denotes the unit vector \mathbf{r}/r . In uniaxially symmetric phases, only real coefficients with $m_1 + m_2 + m = 0$ and even $l_1 + l_2 + l$

enter the expansion. Since our particles have uniaxial symmetry, every single l_i is even as well.

The expansion coefficients of the pair distribution function can be determined directly from the simulations⁴⁶

$$\begin{aligned} \rho_{l_1 m_1 l_2 m_2 l m}^{(2)}(r) = 4\pi \varrho^2 g(r) \\ \langle Y_{l_1 m_1}^*(\mathbf{u}_1) Y_{l_2 m_2}^*(\mathbf{u}_2) Y_{l m}^*(\hat{\mathbf{r}}) \rangle_{\delta r}, \end{aligned} \quad (10)$$

where the average $\langle \cdot \rangle_{\delta r}$ is performed over all molecule pairs at distances $|\mathbf{r}_1 - \mathbf{r}_2| \in [r, r + \delta r]$, and $g(r)$ is the radial distribution function, i. e., the average total number of molecule pairs divided by $N4\pi\varrho r^2 \delta r$. The coordinate frame was determined separately in each configuration, such that the z axis is given by the direction of the director (director frame). In general, we have determined coefficients for values of l, l_i up to $l_{\max} = 6$. For the highest density⁴², we checked in small systems that the truncation is sufficient by comparing the results with those obtained using $l_{\max} = 8$. The bin size was $\delta r = 0.04\sigma_0$ and only ranges up to $r_{\max} = 0.4L$ (L being the size of the simulation box) were considered in order to reduce boundary effects⁴⁷.

The total correlation function h is obtained from the spherical harmonics version of eqn. (6), which is simply a matrix equation:

$$\begin{aligned} \rho_{l_1 m_1 l_2 m_2 l m}^{(2)}(r) = \varrho^2 \left(\sqrt{4\pi} f_{l_1} f_{l_2} \delta_{m_1 0} \delta_{m_2 0} \delta_{l 0} \delta_{m 0} \right. \\ \left. + \sum_{\substack{l'_1, l'_2, l'' \\ l'_1, l'_2, l''}} h_{l'_1 m'_1 l'_2 m'_2 l m}(r) f_{l'_1} f_{l'_2} \Gamma_{m_1 m_1 0}^{l'_1 l'_1 l''} \Gamma_{m_2 m_2 0}^{l'_2 l'_2 l''} \right), \end{aligned} \quad (11)$$

with

$$\Gamma_{mm'm''}^{l'l'l''} = \int d\mathbf{u} Y_{lm}^*(\mathbf{u}) Y_{l',m'}(\mathbf{u}) Y_{l'',m''}(\mathbf{u}) \quad (12)$$

The DCF c is most easily calculated in Fourier representation. The expansion coefficients of a function $F(\mathbf{u}_1, \mathbf{u}_2, \mathbf{r})$ in real space are related to their counterparts in Fourier space by the Hankel transform³

$$F_{l_1 m_1 l_2 m_2 l m}(k) = 4\pi i^l \int_0^\infty r^2 j_l(kr) F_{l_1 m_1 l_2 m_2 l m}(r) dr \quad (13)$$

$$F_{l_1 m_1 l_2 m_2 l m}(r) = \frac{4\pi(-i)^l}{(2\pi)^3} \int_0^\infty k^2 j_l(kr) F_{l_1 m_1 l_2 m_2 l m}(k) dk \quad (14)$$

where $j_l(kr)$ is the spherical Bessel function. The Ornstein-Zernike equation (7) in Fourier space and spherical harmonics representation reads

$$\begin{aligned} h_{l_1 m_1 l_2 m_2 l m}(k) = c_{l_1 m_1 l_2 m_2 l m}(k) \\ + \varrho \sum_{\substack{l_3, l'_3, l''_3 \\ l'_3, l''_3, l''_3}} c_{l_1 m_1 l_3 m_3 l'_3 m'_3}(k) h_{l_3 m_3 l_2 m_2 l''_3 m''_3}(k) \\ \times f_{l'_3}^{l''_3}(-1)^{m_3} \Gamma_{mm'm''}^{l'l'l''} \Gamma_{m_3 m_3 0}^{l'_3 l'_3 l''_3}, \end{aligned} \quad (15)$$

which is again a matrix equation.

Special care must be taken when performing the Hankel transform (13) in the nematic state: Due to the elasticity of the nematic fluid, certain coefficients of h (in particular those with $m_1, m_2 = \pm 1$) have pronounced long-range tails and exhibit a $1/r$ behavior at large distances r . Furthermore, large-wavelength fluctuations are suppressed in finite systems, and the director frame follows the local order if evaluated in a small box. As a result, some coefficients (those with $l = 0, m_i = \pm 1$) are shifted towards zero in finite systems by an amount which is almost constant beyond $r = \sigma_0$ (see Figure 1). Before performing the Hankel transform, we thus fit the data points beyond distances $r > r_0$ to a power law $a + b/r$, shift $h(r)$ by a , and extrapolate it to infinity. At the highest density $\rho = 0.3/\sigma_0^3$, we have simulated systems of different size ($N = 1000, N = 4000$, and $N = 8000$) and checked that finite size effects are basically eliminated by our procedure. The parameter r_0 was chosen $r_0 = 4.0/\sigma_0$ at $N = 4000$, $r_0 = 2.8/\sigma_0$ at $N = 1000$, and $r_0 = 5.3/\sigma_0$ at $N = 8000$.

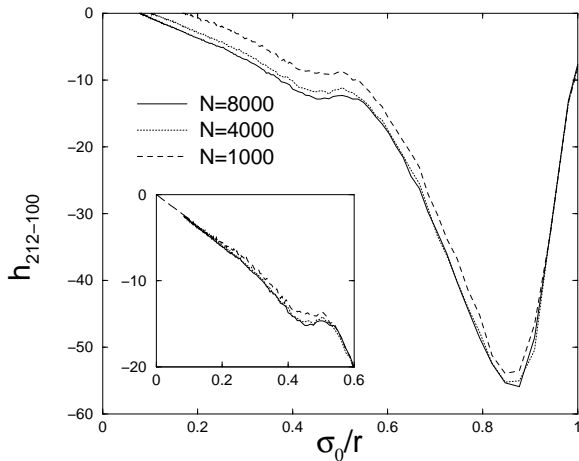


FIG. 1. Expansion coefficient $h_{212-100}$ of the total correlation function vs. $1/r$ for systems of different size at density $\rho = 0.3\sigma_0^{-3}$. Before performing a Hankel transform of this curve, the tails are fitted with a function $a + b/r$, and the whole curve is shifted by a . Inset shows the shifted data. The curves for the two larger systems are then almost on top of each other.

The data manipulations which finally yield the DCF are altogether quite extensive. An independent test of the results which checks the procedure is clearly desirable. For example, one can calculate the elastic constants from the DCF using the Poniewierski-Stecki relations⁴⁰, and compare them with values obtained independently from the structure factor. As we have reported in our earlier paper⁴², the agreement is quite satisfactory. As another test, we have verified the validity of a relation originally derived by Gubbins³¹,

$$\frac{\rho^{(1)'}(u_{1,z})}{\rho^{(1)}(u_{1,z})} u_{1,\alpha} = \int c(\mathbf{u}_1, \mathbf{u}_2, \mathbf{k})|_{k=0} \rho^{(1)'}(u_{2,z}) u_{2,\alpha} d\mathbf{u}_2. \quad (16)$$

In Fourier space and spherical harmonics representation, this reads

$$\begin{aligned} & \sqrt{l(l+1)} \int \ln(\rho^{(1)}(\mathbf{u})) Y_{l0}(\mathbf{u}) d\mathbf{u} \\ &= -\frac{\rho}{2\sqrt{\pi}} \sum_{l'} \sqrt{l'(l'+1)} f_{l'l-100}(k)|_{k=0}. \end{aligned} \quad (17)$$

The quantity on the right hand side of this equation is plotted as a function of k^2 for $l = 2$ and $l = 4$ in Figure 2. The $k \rightarrow 0$ limit agrees well with the value obtained from the left hand side.

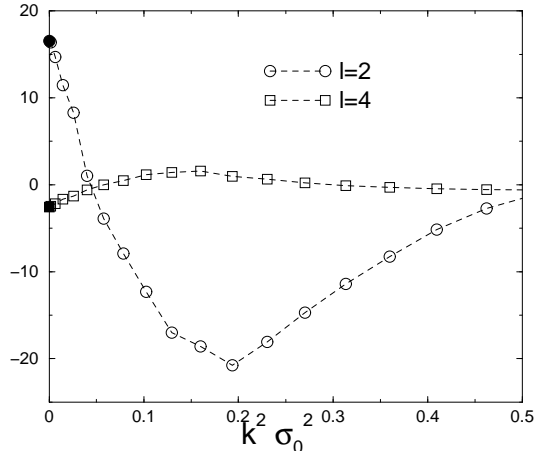


FIG. 2. Illustration of the Gubbins equation (17) for $l = 2$ and 4 at the density $\rho = 0.3\sigma_0^{-3}$. Open symbols show right hand side of eqn. (17) vs. k^2 , closed symbols the value at $k \rightarrow 0$ obtained from the left hand side. The system size was $N = 8000$.

III. RESULTS

The orientational average of the pair correlation functions is shown in Figure 3 for different densities. It is basically given by their respective spherical harmonics coefficients with $l, l_i, m, m_i = 0$. The pair distribution function $\rho^{(2)}$ exhibits several peaks at distances slightly larger than σ_0 , corresponding to the nearest neighbor shell, the next nearest neighbor shell etc. The peaks are less pronounced, but still present in the total correlation function. They disappear in the DCF. At low density, the DCF vanishes at distances beyond $\kappa\sigma_0$. At large densities, however, one observes broad oscillations which persist further. Orientationally averaged, the structure of the DCF does not appear to be much simpler than that of the pair distribution function.

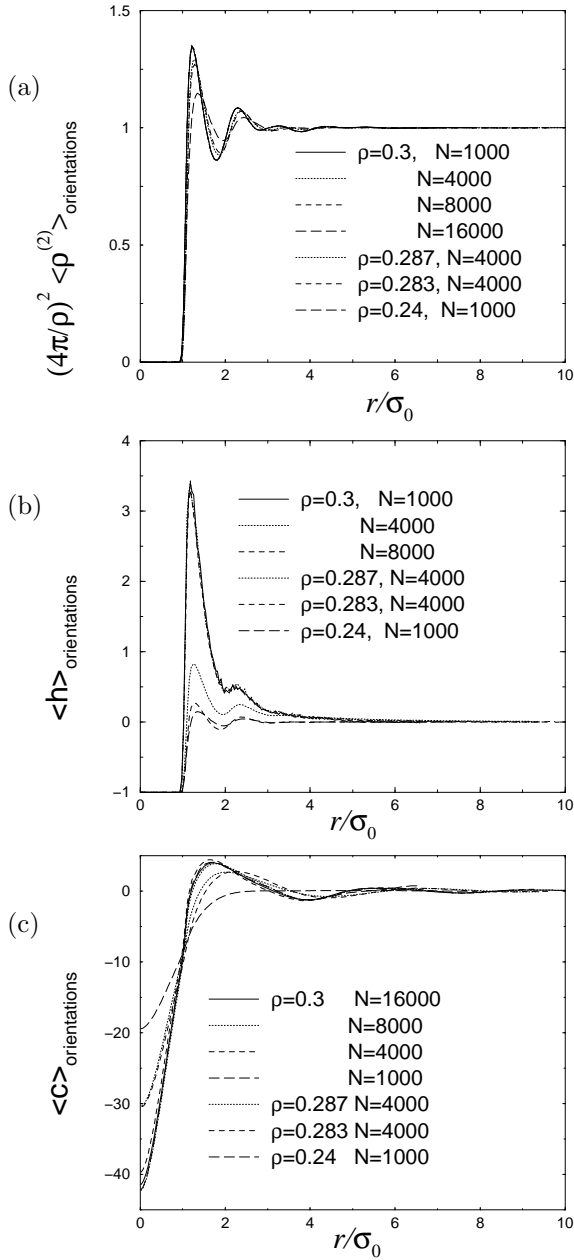


FIG. 3. Orientational average of the pair distribution function $\rho^{(2)}$ (a), the total correlation function h (b), and the direct correlation function c (c) vs. distance r for different densities. Data for different system sizes ($\rho = 0.3\sigma_0^{-3}$) lie on top of each other.

The qualitative difference between the DCF and the total correlation function becomes apparent when looking at coefficients which reflect the elasticity of the nematic fluid. Figure 4 shows as an example the coefficients with $l_1 = l_2 = l = 2$, $m_1 = -m_2 = 1$ and $m = 0$. In the nematic phase, they decay at long distance like $1/r$, both for the pair distribution function and the total pair cor-

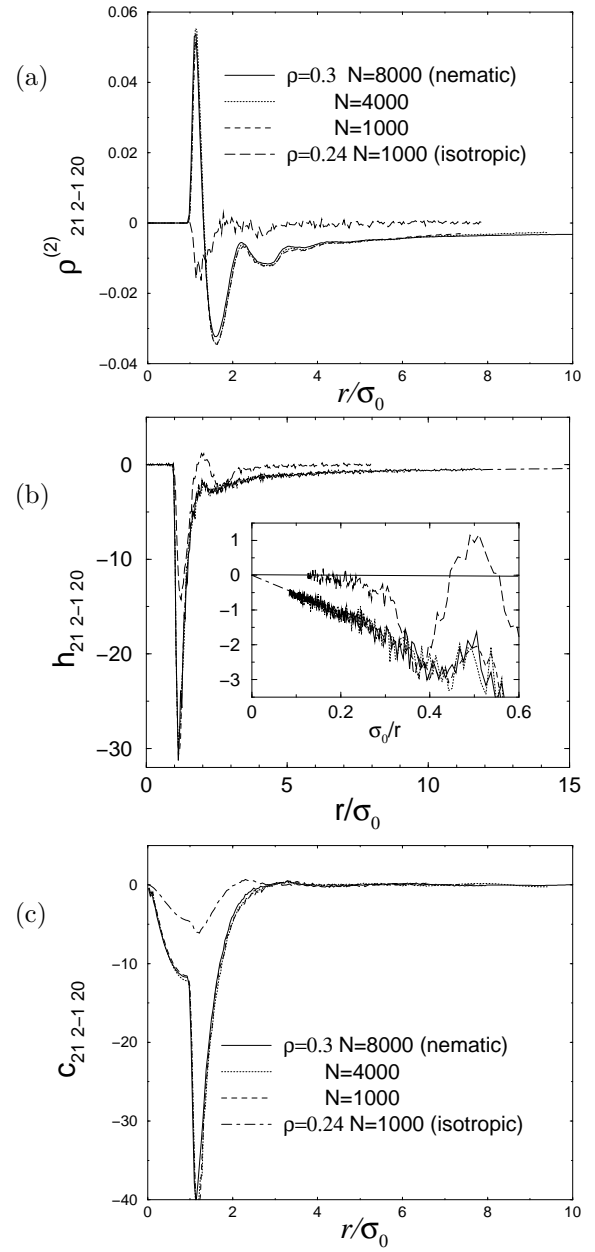


FIG. 4. Expansion coefficient with $l_i = l = 2$ and $m_1 = -m_2 = 1$ of the pair distribution function $\rho^{(2)}$ (a), the total correlation function h (b), and the direct correlation function c (c) vs. distance r for the density $\rho = 0.24\sigma_0^{-3}$ (long dashed line) and $\rho = 0.3\sigma_0^{-3}$ (solid line: system size $N = 8000$, dotted line: $N = 4000$, short dashed line: $N = 1000$). Dashed dotted line in the plot for h indicates extrapolation with a $1/r$ behavior. Inset shows data for h as a function of $1/r$.

relation function. The DCF no longer exhibits such a long ranged tail. Thus the DCF is indeed a quantity which characterizes the structure of nematic fluids on a local scale.

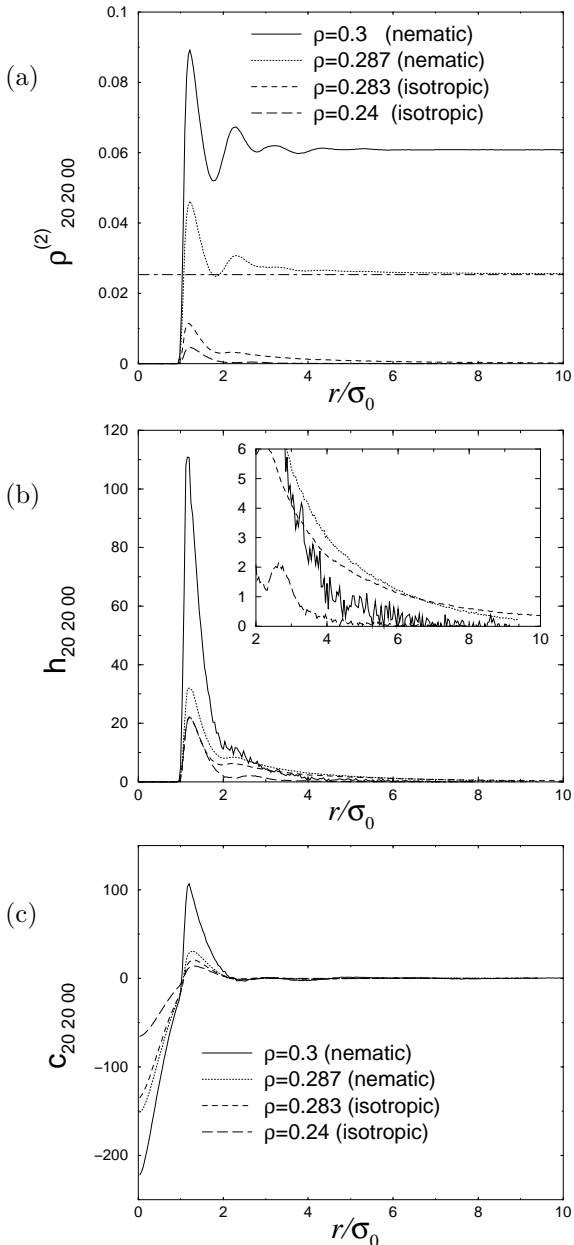


FIG. 5. Expansion coefficient with $l_i = 2$ and $l = m_i = m = 0$ of the pair distribution function $\rho^{(2)}$ (a), the total correlation function h (b), and the direct correlation function c (c) vs. distance r for different densities. Dot dashed line in the plot for $\rho^{(2)}$ indicates infinite range limit for $\rho = 0.287\sigma_0^{-3}$. Inset of (b) shows blowup of data for large distances.

Next we investigate the isotropic/nematic transition in more detail. Figure 5 illustrates how orientational order emerges and gives rise to a constant long range contribution to the pair distribution function coefficients with $l_i \neq 0, m_i = l = m = 0$. The constant contribution is subtracted in the total correlation function (cf. eqn. (6)). Close to the transition, however, the total correla-

tion function features a slowly decaying, quasi long range tail (Fig. 5 b). It stems from near critical fluctuations with large correlation lengths close to the transition, due to the fact that the transition is only weakly first order. Like the elastic tails, these quasicritical long range tails are no longer present in the DCF.

From the results shown so far (Figs 3, 4, and 5), the effect of nematic ordering on the DCF is not obvious. The influence of nematic symmetry breaking on correlation functions is best studied in a molecular-fixed frame system, which takes full advantage of the symmetries in the isotropic phase and thus allows to assess directly the loss of symmetries in the nematic phase. Following Gray and Gubbins³, we introduce a local coordinate system in which the z axis points in the direction \mathbf{r}_{12} of the intermolecular distance vector (“molecular frame”, see figure 6). The other two axes are chosen such that the x axis lies in the plane spanned by \mathbf{r}_{ij} and the director \mathbf{n} ⁴⁵.

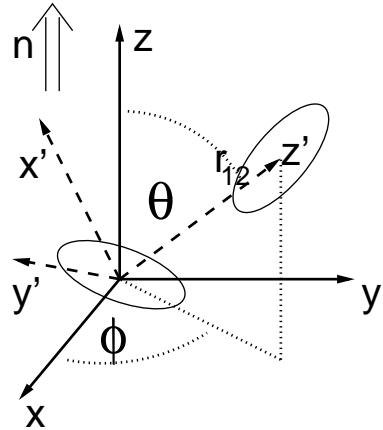


FIG. 6. Illustration of the coordinate frames. Thick solid lines show coordinate axes of director frame, where the z axis points in the direction of the director \mathbf{n} . Thick dashed lines indicate axes of the molecular frame, where the z -axis points along the vector \mathbf{r}_{12} which connects the two particles. The x axis of the molecular frame lies in the plane which is spanned by \mathbf{r}_{12} and \mathbf{n} .

This frame is now used in the spherical harmonics expansion (9) of functions which depend on particle orientations \mathbf{u}_i . The intermolecular distance vector \mathbf{r}_{12} itself is still represented in the director frame. In an isotropic fluid, pair correlation functions must be rotationally invariant, and all expansion coefficients except those with $l = m = 0$ vanish. In a nematic fluid, this is no longer true⁴⁸. Rotational invariance is broken if coefficients with $l \neq 0$ become nonzero. One would certainly expect this to happen for the pair distribution function and the total pair correlation function. In the case of the DCF, the situation is less clear. Zhong and Petschek^{32,35} have argued that the DCF should remain rotationally invariant in an aligned fluid, since it reflects effective pair potentials between particles.

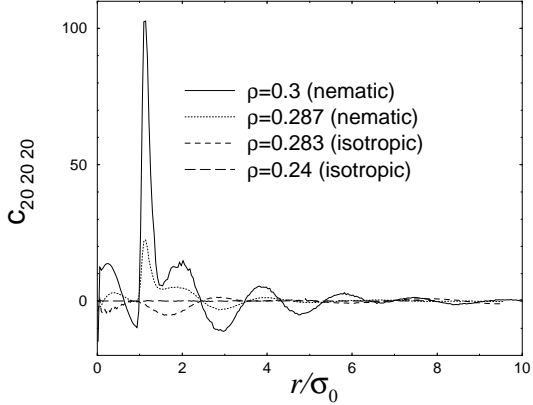


FIG. 7. Expansion coefficient with $l_i = l = 2$ and $m_i = m = 0$ of the direct correlation function in the molecular frame vs. r for different densities. In the isotropic phase, this coefficient must vanish for symmetry reasons. At $\rho = 0.283\sigma_0^{-3}$, a small nonzero remnants are observed due to finite size effects.

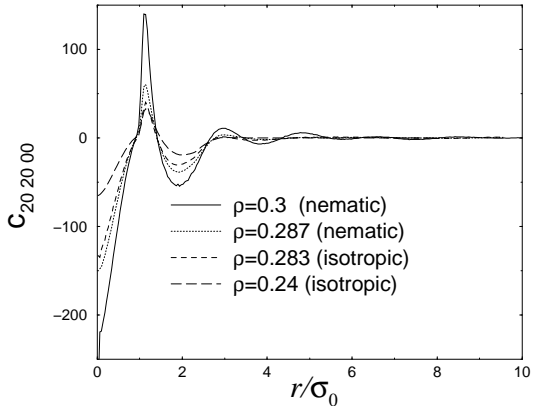


FIG. 8. Expansion coefficient with $l_i = 2$ and $l = m_i = m = 0$ of the direct correlation function in the molecular frame vs. r for different densities.

An equation which converts expansion coefficients from the director frame into the molecular frame is derived in the appendix. Such conversion formulae can be found for isotropic fluids in the literature³. Our general case is more involved.

Figure 7 shows an example of an expansion coefficient, c_{202020} , which vanishes in the case of rotational invariance. In the isotropic phase, the values are indeed close to zero. In the nematic phase, a nonzero DCF coefficient not only emerges, it may even grow quite large. At $\rho = 0.3\sigma_0^{-3}$ the values are comparable to those of a symmetry preserving coefficient of similar order (8). Hence the DCF reflects the broken symmetry in the nematic

phase. Zhong's and Petschek's seemingly reasonable assumption is not valid for fluids of ellipsoids.

In contrast, the symmetry preserving coefficient c_{202000} seems barely affected by the transition (Fig. 8). The curves for $\rho = 0.283\sigma_0^{-3}$ and $\rho = 0.287\sigma_0^{-3}$, slightly below and above the transition, lie almost on top of each other.

It is instructive to compare the simulation results for the DCF with the results from the Percus-Yevick theory⁴. In the Percus-Yevick approximation, the direct correlation function is determined by the Ornstein-Zernike equation (7) and the additional closure relation

$$c(\mathbf{u}_1, \mathbf{u}_2, \mathbf{r}_{12}) = (1 - e^{V_{12}/k_B T}) (h(\mathbf{u}_1, \mathbf{u}_2, \mathbf{r}_{12}) + 1), \quad (18)$$

where V_{12} is the pair potential between the particles 1 and 2. In a homogeneous isotropic fluid, this defines a closed set of equations. In an orientationally fluid, one needs an additional condition for the one particle distribution $\rho^{(1)}(\mathbf{u})$, e. g., eqn. (16).

We have calculated the DCF in Percus-Yevick approximation for the density values of our simulation. We followed the procedure described by Letz and Latz¹³, except that we imposed eq. (16) instead of isotropy. Nevertheless, we only obtained isotropic solutions. This is consistent with an argument of Zhong and Petschek, who showed that the diagrammatic expansion of the Ward identity, an equation related to (16), must contain diagrams in the anisotropic case which are excluded by the Percus-Yevick closure³². Thus the Percus-Yevick closure is probably not compatible with spontaneous orientational ordering.

In the Percus-Yevick calculations, the spherical harmonics expansion was extended up to $l_{\max} = 4$. In addition, we have also performed systematic calculations with $l_{\max} = 2$. Here we observed an interesting scenario: Over a wide range of densities, two solutions exist that meet in a bifurcation at an upper critical density ρ_c and disappear beyond ρ_c . One of the branches merges into the Onsager solution at low densities. The other yields much more structured correlation functions and is clearly unphysical. Unfortunately, we have not been able to analyze systematically the situation at higher cutoff l_{\max} . Our results suggest that the scenario at $l_{\max} = 4$ might be similar. (For example, we found two solutions at $\rho = 0.29\sigma_0^{-3}$). Therefore it may well be that the behavior observed at $l_{\max} = 2$ is a generic-feature of the Percus-Yevick approximation and not an artefact of the truncation of l . This would explain how the Percus-Yevick solution can disappear at high densities without exhibiting a nematic instability¹⁸.

Figure 9 compares the Percus-Yevick prediction for the DCF coefficient with $l_i = 2, l = m = m_i = 0$ with the simulation data for densities $\rho = 0.24\sigma_0^{-3}$ and $\rho = 0.283\sigma_0^{-3}$. The agreement is good even for the higher density, which is just below the transition. Above the transition, we can contrast the DCF with the Percus-Yevick solution for the isotropic fluid of the same density. For example, the Percus-Yevick DCF for $\rho = 0.3\sigma_0^{-3}$,

shown in figure 9 b), can be compared with the real DCF, shown in figure 8. The agreement is not very good. The real, nematic DCF exhibits much more structure than the Percus-Yevick result.

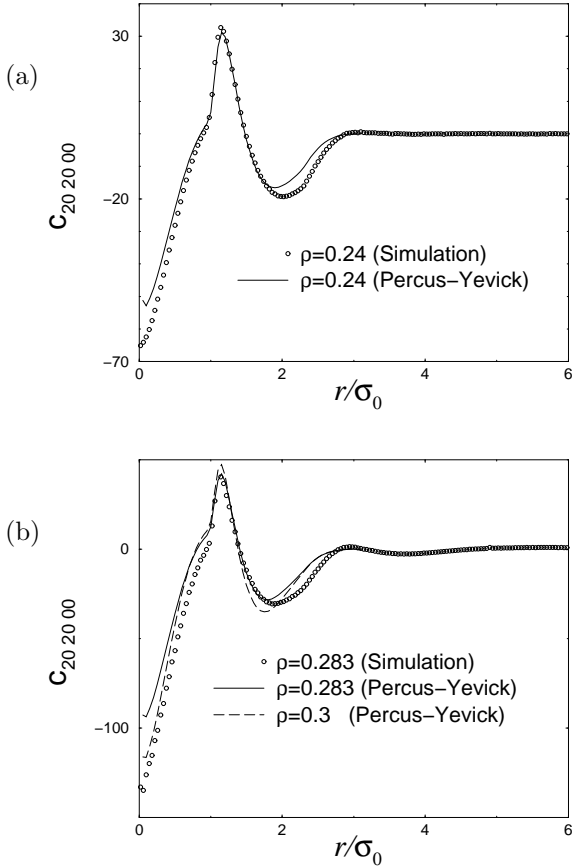


FIG. 9. Expansion coefficient with $l_i = 2$ and $l = m_i = m = 0$ of the direct correlation function in the molecular frame vs. distance r in Percus-Yevick approximation and in simulations at the density $\rho = 0.24\sigma_0^{-3}$ (a) and $\rho = 0.283\sigma_0^{-3}$ (b). Simulation data are the same as in fig. 8. (same data as figure 8). Dashed line shows Percus-Yevick prediction for $\rho = 0.3\sigma_0^{-3}$ for comparison.

IV. SUMMARY AND CONCLUSIONS

To summarize, we have studied the local structure of fluids of uniaxial ellipsoids at different densities in the vicinity of the nematic/isotropic phase transition. In particular, we have calculated and analyzed the DCF. We find that the DCF suitably characterizes the local structure, in the sense that it is short ranged both in the isotropic and the nematic phase. This reflects the short range nature of the interactions in our model. In other respect, however, the DCF does not reproduce the properties of the pair interaction potential. Notably, it

loses rotational invariance in the nematic phase and features a substantial symmetry breaking contribution. In contrast, the symmetry preserving part of the DCF does not change dramatically at the nematic/isotropic transition.

Our results should be useful guides for future developments of density functional theories for anisotropic fluids⁴⁹, or of improved liquid state theories for nematic liquids in general. Moreover, we can use the DCF directly to predict the structure of inhomogeneous fluids of ellipsoids within simple density functional or integral equation approaches¹. Such work is currently under way.

ACKNOWLEDGMENTS

We thank M. P. Allen, G. Germano, and H. Lange for fruitful interactions. Some of the simulation data analyzed here have already been discussed in Ref.⁴². These were produced in part by G. Germano, using a parallel MD program GBMEGA originally developed by the EP-SRC Complex Fluids Consortium, UK. Both for the simulations and the analyses, we have made extensive use of the CRAY T3E of the HLRZ in Jülich. This work was supported from the German Science Foundation (DFG).

APPENDIX

In this appendix, we derive an equation which allows to convert expansion coefficients of pair correlation functions from the director frame to the molecular frame.

We denote by $F^{dir}(\mathbf{u}_1, \mathbf{u}_2, \mathbf{r})$ and $F^{mol}(\mathbf{u}'_1, \mathbf{u}'_2, \mathbf{r})$ the representation of a correlation function F in the director frame and the molecular frame, respectively. These are expanded in spherical harmonics according to eqn. (9), hence

$$F^{dir}(\mathbf{u}_1, \mathbf{u}_2, \mathbf{r}) = \sum_{\substack{l_1, l_2, l \\ m_1, m_2, m}} F_{l_1 m_1 l_2 m_2 l m}^{dir}(r) Y_{l_1 m_1}(\mathbf{u}_1) Y_{l_2 m_2}(\mathbf{u}_2) Y_{lm}(\hat{\mathbf{r}}), \quad (19)$$

and

$$F_{l'_1 m'_1 l'_2 m'_2 l' m'}^{mol}(r) = \int d\mathbf{u}_r d\mathbf{u}'_1 d\mathbf{u}'_2 F^{mol}(\mathbf{u}'_1, \mathbf{u}'_2, \mathbf{r}) Y_{l'_1 m'_1}^*(\mathbf{u}'_1) Y_{l'_2 m'_2}^*(\mathbf{u}'_2) Y_{l' m'}^*(\mathbf{u}_r). \quad (20)$$

Now let $\mathcal{R}(\Omega) \equiv \mathcal{R}(\theta, \phi, \chi)$ be the rotation operator which carries the director frame into coincidence with the molecular frame (see figure 6),

$$F^{mol}(\mathbf{u}'_1, \mathbf{u}'_2, \mathbf{r}) = F^{dir}(\mathcal{R}\mathbf{u}'_1, \mathcal{R}\mathbf{u}'_2, \mathbf{r}). \quad (21)$$

The angles θ and ϕ are the polar coordinates of the intermolecular distance vector \mathbf{r}_{ij} in the director frame, and $\chi = \pi$. The coefficients of F in the director frame and in the molecular frame are then related to each other by

$$F_{l_1' m_1' l_2' m_2' l' m'}^{mol}(r) = \sum_{\substack{l_1, l_2, l \\ m_1, m_2, m}} K_{l_1 m_1 l_2 m_2 l m}^{l_1' m_1' l_2' m_2' l' m'} F_{l_1 m_1 l_2 m_2 l m}^{dir}(r), \quad (22)$$

where $K_{l_1 m_1 l_2 m_2 l m}^{l_1' m_1' l_2' m_2' l' m'}$ is given by

$$K_{l_1 m_1 l_2 m_2 l m}^{l_1' m_1' l_2' m_2' l' m'} = \int d\mathbf{u}_r d\mathbf{u}_1' d\mathbf{u}_2' Y_{l_1' m_1'}^*(\mathbf{u}_1') Y_{l_2' m_2'}^*(\mathbf{u}_2') \times Y_{l' m'}^*(\mathbf{u}_r) Y_{l_1 m_1}(\mathcal{R}\mathbf{u}_1') Y_{l_2 m_2}(\mathcal{R}\mathbf{u}_2') Y_{lm}(\mathbf{u}_r). \quad (23)$$

Next we apply the transformation formula³

$$Y_{l_1 m_1}(\mathcal{R}\mathbf{u}_1') = \sum_M D_{m_1 M}^{l_1}(\Omega)^* Y_{l_1 M}(\mathbf{u}_1'), \quad (24)$$

where $D_{m_1 M}^{l_1}(\Omega)$ is the rotation matrix of the operator \mathcal{R} , given by

$$D_{mn}^l(\theta, \phi, \chi) = e^{-im\phi} \sum_k (-1)^k \left(\frac{1}{2}\right)^l C_{lmnk} \times (1+a)^{l-k+\frac{m-n}{2}} (1-a)^{k-\frac{m-n}{2}} e^{-in\chi} \quad (25)$$

with $a = \cos\theta$ and

$$C_{lmnk} = \frac{\sqrt{(l+m)!(l-m)!(l+n)!(l-n)!}}{(l+m-k)!(l-n-k)!k!(k-m+n)!}. \quad (26)$$

The sum over k is taken over values such that the arguments of the factorials in the denominator of C_{lmnk} are positive, i.e., $\max(0, m-n) \leq k \leq \min(l-n, l+m)$. Eq. 23 then becomes

$$K_{l_1 m_1 l_2 m_2 l m}^{l_1' m_1' l_2' m_2' l' m'} = \int d\mathbf{u}_r Y_{l' m'}^*(\mathbf{u}_r) Y_{lm}(\mathbf{u}_r) D_{m_1 m_1'}^{l_1}(\Omega)^* \delta_{l_1 l_1'} D_{m_2 m_2'}^{l_2}(\Omega)^* \delta_{l_2 l_2'}. \quad (27)$$

Using eqn. (25) with $\chi = \pi$ and the relation

$$Y_{lm} = \sqrt{\frac{(2l+1)(l-m)!}{4\pi(l+m)!}} e^{im\phi} P_{lm}(a), \quad (28)$$

(P_{lm} is the associated Legendre polynomial), we obtain

$$K_{l_1 m_1 l_2 m_2 l m}^{l_1' m_1' l_2' m_2' l' m'} = \delta_{l_1 l_1'} \delta_{l_2 l_2'} \delta_{m_1+m_2+m, m'} (-1)^{m'+m_2'} \times \left(\frac{1}{2}\right)^{l_1+l_2} \sqrt{(2l_1+1)(2l_2+1)} \sqrt{\frac{(l-m)!(l'-m')!}{(l+m)!(l'+m')!}} \times \sum_{k_1, k_2} (-1)^{k_1+k_2} C_{l_1 m_1 m_1' k_1} C_{l_2 m_2 m_2' k_2} \times \frac{1}{2} \int_{-1}^1 da P_{l' m'}(a) P_{lm}(a) (1+a)^{l_1+l_2} \times \sqrt{(1-a)/(1+a)}^{(-m_1'-m_2'+m_1+m_2+2k_1+2k_2)}.$$

In a uniaxial nematic phase, molecular frame coefficients with $m' \neq 0$ must vanish. Thus eqn. (29) reduces to

$$K_{l_1 m_1 l_2 m_2 l m}^{l_1' m_1' l_2' m_2' l' m'} = \delta_{l_1 l_1'} \delta_{l_2 l_2'} \delta_{m_1+m_2+m, 0} \times \left(\frac{1}{2}\right)^{l_1+l_2} \sqrt{(2l_1+1)(2l_2+1)} \sqrt{\frac{(l-m)!}{(l+m)!}} \times \sum_{k_1, k_2} (-1)^{k_1+k_2} C_{l_1 m_1 m_1 k_1} C_{l_2 m_2 m_2 k_2} \times \frac{1}{2} \int_{-1}^1 da P_{l'}(a) P_{lm}(a) (1+a)^{l_1+l_2} \times \sqrt{(1-a)/(1+a)}^{2k_1+2k_2+m_1'+m_2'} (-1)^{m_1'+m_2'} \quad (30)$$

In an isotropic phase, one can use this result with $l' = m' = 0$ and $m_1' = -m_2' = \bar{m}$.

The matrix for the inverse transformation from the molecular frame to the director frame the same, eqn. (30). We have performed several numerical tests to check this result: Pair distribution functions were determined from the simulation data both in the molecular frame and in the director frame. Then we applied the transformation formula and checked that the result is the same⁵⁰. In another test, we have transformed correlation functions into the molecular frame and back again, and compared the result with the original data.

-
- ¹ J. P. Hansen and I. R. McDonald, *Theory of Simple Liquids* (Academic Press, London, 1986).
 - ² R. Evans, in *Fundamentals of Inhomogeneous Fluids*, p. 86, D. Henderson ed. (Marcel Dekker, New York, 1992).
 - ³ C. G. Gray and K. E. Gubbins, *Theory of Molecular Fluids*, Vol. 1 (Oxford, New York, 1984).
 - ⁴ J. E. Percus and G. J. Yevick, Phys. Rev. **110**, 1 (1958).
 - ⁵ R. Pynn, Solid State Comm. **14**, 29 (1974).
 - ⁶ Y. Chen and W. A. Steele, J. Chem. Phys. **54**, 703 (1971).
 - ⁷ A. Wulf, J. Chem. Phys. **55**, 4512 (1971).
 - ⁸ P. H. Fries and G. N. Patey, J. Chem. Phys. **82**, 429 (1985); J. Chem. Phys. **85**, 7007 (1986).
 - ⁹ R. C. Singh, J. Ram, Y. Singh, Phys. Rev. E **54**, 977 (1996).
 - ¹⁰ A. Perera, P. G. Kusalik, and G. N. Patey, Mol. Phys. **60**, 77 (1987); J. Chem. Phys. **87**, 1295 (1987); *ibid* **89**, 5969 (1988); A. Perera and G. N. Patey, J. Chem. Phys. **89**, 5861 (1988); J. Talot, A. Perera, and G. N. Patey, Mol. Phys. **70**, 285 (1990).
 - ¹¹ R. Pospisil, A. Malijevsky, W. R. Smith, Mol. Phys. **79**, 1011 (1993).
 - ¹² J. Ram, Y. Singh, Phys. Rev. A **44**, 3718 (1991); J. Ram, R. C. Singh, Y. Singh, Phys. Rev. E **49**, 5117 (1994); S. Gupta, J. Ram, R. C. Singh, Physica A **278**, 447 (2000).
 - ¹³ M. Letz and A. Latz, Phys. Rev. E **60**, 5865 (1999).
 - ¹⁴ A. Wulf, J. Chem. Phys. **71**, 104 (1979).
 - ¹⁵ G. Rickayzen, Mol. Phys. **75**, 333 (1992); M. Calleja and G. Rickayzen, Mol. Phys. **76**, 693 (1992); P. Kalpaxis and G. Rickayzen, Mol. Phys. **80**, 391 (1993).
 - ¹⁶ M. Calleja and G. Rickayzen, Phys. Rev. Lett. **74**, 4452 (1995); J. Phys.: Cond. Matt. **7**, 8839 (1995).
 - ¹⁷ G. Rickayzen and M. Calleja, Mol. Phys. **90**, 869 (1997); G. Rickayzen, Mol. Phys. **95**, 393 (1998).

- ¹⁸ A. Chamoux and A. Perera, J. Chem. Phys. **104**, 1493 (1995); Phys. Rev. E **58**, 1933 (1998).
- ¹⁹ Y. Rosenfeld, Phys. Rev. Lett. **63**, 980 (1989).
- ²⁰ A. Wulf, J. Chem. Phys. **67**, 2254 (1977).
- ²¹ J. D. Parsons, Phys. Rev. A **19**, 1125 (1979).
- ²² S.-D. Lee, J. Chem. Phys. **87**, 4972 (1987).
- ²³ M. Baus, J.-L. Colot, X.-G. Wu, H. Xu, Phys. Rev. Lett. **59**, 2184 (1987).
- ²⁴ J. F. Marko, Phys. Rev. A **39**, 2050 (1989).
- ²⁵ M. P. Allen, C. P. Mason, E. de Miguel, J. Stelzer, Phys. Rev. E **52**, R25 (1995).
- ²⁶ J. G. Gay and B. J. Berne, J. Chem. Phys. **74**, 3316 (1981).
- ²⁷ M. P. Allen, J. T. Brown, and M. A. Warren, J. Phys.: Cond. Matter **8**, 9433 (1996).
- ²⁸ M. P. Allen and M. A. Warren, Phys. Rev. Lett. **78**, 1291 (1997).
- ²⁹ P.-G. de Gennes and J. Prost, *The Physics of Liquid Crystals* (Oxford University Press, Oxford, 1995).
- ³⁰ S. Chandrasekhar, *Liquid Crystals* (Cambridge University Press, Cambridge, 1992).
- ³¹ K. E. Gubbins, Chem. Phys. Lett. **76**, 329 (1980).
- ³² H. Zhong, R. G. Petschek, Phys. Rev. E **51**, 2263 (1994).
- ³³ H. Workman and M. Fixman, J. Chem. Phys. **58**, 5024 (1973).
- ³⁴ J. M. Caillol, J. J. Weis, and G. N. Patey, Phys. Rev. A **38**, 4772 (1988); J. M. Caillol and J. J. Weis, J. Chem. Phys. **90**, 7403 (1989).
- ³⁵ H. Zhong, R. G. Petschek, Phys. Rev. E **53**, 4944 (1995).
- ³⁶ M. F. Holovko, T. G. Sokolovska, J. Mol. Liq. **82**, 161 (1999).
- ³⁷ J. Stelzer, L. Longa, and H. R. Trebin J. Chem. Phys. **103**, 3098 (1995); *ibid* **107**, 1295 (1997); Mol. Cryst. Liq. Cryst. **262**, 455 (1995); J. Stelzer, M. A. Bates, L. Longa, and G. R. Luckhurst, J. Chem. Phys. **107**, 7483 (1997).
- ³⁸ A. V. Zakharov and A. Maliniak, Eur. Phys. J. E **4**, 85 (2001).
- ³⁹ L. Longa, G. Cholewiak, R. Trebin, G. R. Luckhurst, Eur. Phys. J. E **4**, 51 (2001).
- ⁴⁰ A. Poniewierski, J. Stecki, Mol. Phys. **38**, 1931 (1979).
- ⁴¹ M. P. Allen, M. A. Warren, M. R. Wilson, A. Sauron, and W. Smith, J. Chem. Phys. **105**, 2850 (1996).
- ⁴² N. H. Phuong, G. Germano, and F. Schmid, J. Chem. Phys. **115**, 7227 (2001).
- ⁴³ B. J. Berne and P. Pechukas, J. Chem. Phys. **56**, 4213 (1975).
- ⁴⁴ H. Lange and F. Schmid, J. Chem. Phys. **117**, 362 (2002); Comp. Phys. Comm. **147**, 276 (2002).
- ⁴⁵ In the isotropic phase, a “director” obviously does not exist. The choice of the coordinate system is then arbitrary. For reasons of consistency, we still use the Eigenvector corresponding to the (small) largest Eigenvalue of the order tensor \mathbf{Q} .
- ⁴⁶ W. B. Streett and D. J. Tildesley, Proc. Roy. Soc. Lond. A **348**, 485-510 (1975).
- ⁴⁷ L. R. Pratt and S. W. Haan, J. Chem. Phys. **74**, 1873 (1980).
- ⁴⁸ Some restrictions still remain in uniaxial nematic fluids: All molecular frame coefficients are real and vanish unless $m = 0$ and $l_1 + l_2$ is even. In our case, l_1 and l_2 must also be even individually because of the symmetry of the particles.
- ⁴⁹ G. Cinacchi and F. Schmid, J. Phys.: Cond. Matter **14**, 12223 (2002); G. Cinacchi and F. Schmid, in preparation.
- ⁵⁰ Nguyen H. Phuong, Dissertation Universität Bielefeld (2002).